

# Heat pipes with variable thermal conductance property developed for space applications

V. Kravets<sup>1</sup>, Ye. Alekseik<sup>1\*</sup>, O. Alekseik<sup>1</sup>, S. Khairnasov<sup>1</sup>, V. Baturkin<sup>2</sup>, T. Ho<sup>2</sup>, L. Celotti<sup>3</sup>

<sup>1</sup> Heat Pipes Laboratory of Heat-and-power engineering faculty, National Technical University of Ukraine "Kyiv polytechnic institute", Kyiv, 03056 Ukraine,

<sup>2</sup> DLR Institut für Raumfahrtsysteme, Explorationssysteme RY-ES, Bremen, 28359 Germany,

<sup>3</sup> Active Space Technologies GmbH, Berlin, 12489 Germany.

---

## Abstract

The activities presented in this paper focus on a new approach to provide passive regulation of the electronic unit thermal regime of the MASCOT lander (DLR) onboard the NEA sample return mission Hayabusa 2 (JAXA), by using heat pipes. It provides information on the development and testing of heat pipes with variable thermal conductance in a predetermined temperature range. Such heat pipes acts as thermal switches, but their construction does not include additional elements inherent to gas loaded heat pipes (GLHP) and thermal diode heat pipes (TDHP). Copper heat pipes with metal fibrous wick were chosen as baseline design. We have obtained positive results by choosing heat carrier and structural parameters of wick (i.e. pore diameter, porosity and permeability). A rising of heat pipes thermal conductivity from 0.04 to 2.1 W/K was observed in the temperature range between -20°C...+55°C. The heat pipes transferred predetermined power not less than 10 W within the temperature range of +20°C... +55°C. These heat pipes are in flight since December 2014 and the telemetric data obtained in September 2015 showed normal operation of the thermal control system.

**Keywords:** Heat pipe; Metal fiber; Space applications; Thermal conductance; Wick.

---

## 1. INTRODUCTION

Contemporary aerospace equipment is characterized by a continuous growth of power consumption and increasing of their lifetime. New space satellites designs, from telecommunication satellite to microsatellite, include thermal stabilization systems which are based on heat pipes (HPs) [1]. Heat pipes are devices of very high thermal conductance and have successful heritage in space craft applications.

However the evolution of electronic devices opens new problems with ensuring their thermal modes. Such problems are caused by the need of reliable passive thermal control systems for a narrow range of payload and subsystem operation (e.g., for navigation devices, optical devices and chemical batteries). Moreover the new electronics devices are characterized by high dissipated heat flux.

In this aspect, heat pipes with variable conductance properties such as the thermal diodes heat pipes (TDHP) [2], gas loaded heat pipes (GLHP) [3] and loop heat pipes (LHP) [4] are prime example of solving these issues. The particular application of HPs is the removal of heat from the electronic components and other heat-generating devices on satellites. However the growth of application of HPs with variable conductance properties for space technologies

requires the improvement of their reliability, the simplification of their design, the increase of their efficiency while decreasing weight and overall parameters. Along with the above mentioned HPs with variable conductance, also the usage of constant conductance heat pipes (CCHPs) could be considered. In this case the CCHP technology provides the variable conductance of HPs by the physical properties of their heat carrier and a special combination of the structural parameters of wick (pore diameter, porosity and permeability).

HPs with following heat carriers: methanol (fig. 1a), water (fig. 1b), acetone (fig. 1c) and with thermal properties that vary at the change of the exploitation temperature and applied power, have been developed by the Heat Pipe Laboratory of the National Technical University of Ukraine "Kyiv Polytechnic Institute" (HPL KPI) for the projects Fragment (1980), SKALA (1983), Phobos (1986) and Magion 4, 5 (1995, 1996) (fig. 1) [5].

At that time space practice had not sufficient experience in the usage of these combinations "wick-heat carrier" in thermal control systems (TCS). All HPs are characterized by the relatively small length of the condenser zone ( $L_{\text{con}}/L_{\text{HP}}=0.1...0.22$ ), the profiled wick porosity and thickness along the HPs length. This allowed enlarging the heat transport ability, limited by the HP cross section when compared with the uniform

---

\*Corresponding author: [alexeik\\_kpi@ukr.net](mailto:alexeik_kpi@ukr.net), Phone: +38-063-261-79-59

wick. All designs have demonstrated a sensitivity of the thermal resistance from the applied power and heat output zone temperature. However this feature was not the major requirement for their application although it played a positive role to stabilize heat source temperature.

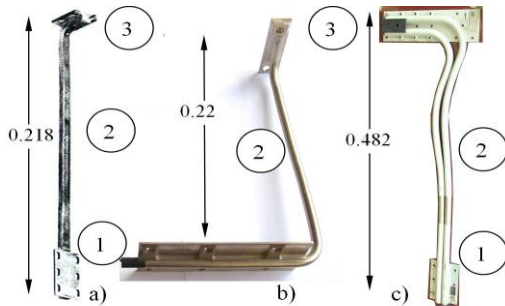


Fig. 1. Heat pipes with variable properties for Project Fragment (a), SKALA (b), Magion 4, 5 (c). 1 – evaporator, 2 – adiabatic, 3 – condenser. Courtesy of KPI.

For the MASCOT project the baseline design were copper heat pipes with metal fibrous wick and methanol as heat carrier. The approach is based on using the peculiarities of conventional HPs, but working in uncharacteristic operational regimes in the space apparatus. These regimes correspond to temperature ranges, which reflect transition modes such as the start-up of heat pipe (at a temperature tending to the freezing point of heat carrier) or the stop operation (at a temperature tending to the triple point of heat carrier). For example, HP operating at inner under pressure promotes the growth of the vapor velocity. The velocity becomes so high, that the vapor carries away heat carrier and locks it in the condensation zone, which leads to HP “OFF”. These regimes are specific for certain heat carrier, which allow varying the “ON/OFF” temperature of the HP for predetermined requirements of the TCS. Additionally, the capability to use the different structural wick parameters allows influencing the variable performances of HPs. Thus, by varying heat carriers (acetone, methanol, ethanol, distilled water, ammonia and etc.) and wick parameters (sizes, porosity, pore diameter) it is possible to create passive TCS of space apparatus with variable heat transfer performances, simplified design and improved efficiency.

Ground tests and the first results of the MASCOT project showed the perspective of such a solution.

## 2. DESCRIPTION OF CURRENT APPLICATION OF HEAT PIPES IN MASCOT

MASCOT (Mobile Asteroid Surface Scout) is a small lander (smaller than  $300 \times 300 \times 200 \text{mm}^3$ ) built by DLR (in collaboration with CNES), embarked on JAXA’s Hayabusa-2 spacecraft, a scientific mission to study the asteroid 162173 Ruygu. During cruise, MASCOT is cradled by a support structure, on the external panel of the main spacecraft, always in the shadow of the high gain antenna. After reaching the target asteroid, MASCOT is released by Hayabusa-2 at a low height (<100 m), lands and starts its scientific investigations on the surface: inspecting the asteroid soil, its composition and characteristics, performing magnetic field measurement, detailed close-up images (fig. 2).

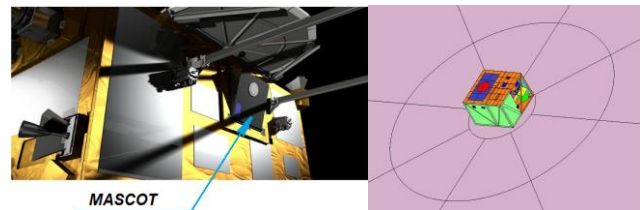


Fig. 2. Left: MASCOT in Hayabusa-2 (artist view) and on the asteroid surface.

As a result of the specific mission phases, contrasting requirements for the thermal control subsystem are present. During the first phase (cruise on-board Hayabusa -2), the lander should limit as much as possible the heat exchange with the S/C and with the environment, while kept above the minimum temperature limits by the survival heaters. During the asteroid phase, the mission duration is directly dependent on the ability of the lander to “stay cool” rejecting the heat produced internally to the outside. Moreover, during cruise, some “switch-ON” phases are foreseen for internal health-checks of the lander. In order to allow these checks, temperature of the whole lander must be raised, increasing the power consumption of the heaters. When the lander is ON, then it must be assured that the internal temperatures do not overcome the maximum limits. This “variable” behavior during cruise can only be obtained via a variable conductance thermal link between the internal major dissipating components of the lander and the external radiator.

The technology presented in this paper was selected as variable thermal conductance link to satisfy all the mission requirements, after

evaluating many possible technologies and their advantages and drawbacks:

- LHP: scalable heat transfer level and start of the heat transfer; a bulky evaporator with respect to the limited internal volume available.
- TDHP: two independent conductance values (cruise and asteroid phase); non maturity of the technology at the beginning of the project.
- Existing commercial GLHP: scalable performances, variable conductance and variable heat transfer levels; presence of a non condensable gas reservoir, increased volume, limited performances.

The technology adopted presents a design similar to the constant conductance heat pipes minimizing the volume occupied (absence of a non-condensable gas reservoir, no bulky evaporator) and the mass, but obtaining a variable conductance effect.

Two heat pipes with slightly different design are implemented between the internal electronic box and the external radiator: type A and B with only differences in routing and shape (fig. 3).

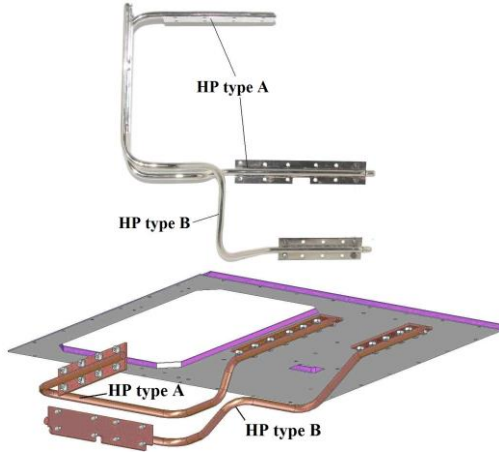


Fig. 3. The MASCOT heat pipes system.

### 3. CHARACTERISTICS OF THE VCHPs FOR THE PROJECT MASCOT

The VCHPs for the project MASCOT were of two types: type A and type B. The difference between these types was only in the mass and the linear dimensions (Table 1).

Both types were made of the copper tubes with outer diameter 6 mm and inner diameter 5 mm. The inner surface of the tubes was covered with the layer of the wick with porosity 82...84%. The equivalent diameter of the vapour space was 3.1 mm. The wick was made of the copper fiber with diameter of

$70 \cdot 10^{-6}$  m and length of 7 mm. Methanol was used as heat carrier. Volume of heat carrier was 6 ml for HP type A and 5 ml for HP type B.

Table 1. The dimensions of the VCHPs for the project MASCOT.

VCHP type	Mass m, kg	Total length L, m	Length of heat input zone $L_{ev}$ , m	Length of heat output zone $L_{con}$ , m
A	0.123	0.482	0.096	0.127
B	0.112	0.438	0.099	0.093

Methanol was chosen as most suitable heat carrier for the operative temperature range of the project MASCOT. Porosity, diameter and length of the fiber mentioned above were chosen in order to obtain extremely low maximum heat transfer ability of the HPs in the temperature range from  $-60^{\circ}\text{C}$  to  $0^{\circ}\text{C}$  and  $10...15$  W – from  $0^{\circ}\text{C}$  to  $+55^{\circ}\text{C}$ .

Maximum heat transfer ability was estimated as the minimal value from the heat transfer abilities specified by the hydrodynamic, the sonic and the boiling crisis limitations in the HPs. These limitations were calculated as [6, 7]:

the hydrodynamic limit (without vapor pressure

$$Q_{\max}^{\text{hyd}} = 2.19 \frac{N \cdot S \cdot F_w}{L_{\text{eff}}} \text{ losses) ,} \quad (1)$$

where  $S$  – the function characterizing the wick

$$S = d_f \left[ \frac{1 - \Pi}{1 + (1 - \Pi)^2} - \frac{1 + \ln(1 - \Pi)}{2 \cdot (1 - \Pi)} \right] \times \left( \frac{1 - \Pi}{1 - \Pi_{\max}} \right)^3 \cdot \exp \left[ -1.45 \cdot \frac{1 - \Pi}{(1 - \Pi_{\max})^{0.7}} \right]; \quad (2)$$

$$L_{\text{eff}} = \frac{L_{\text{ev}} + L_{\text{con}}}{2} + L_{\text{ad}}; \quad (3)$$

the sonic limit

$$Q_{\max}^{\text{sn}} = F_{\text{vc}} \cdot \rho_v \cdot r \cdot \sqrt{\frac{\gamma_v R_{\mu}^v T_s}{2\mu(\gamma_v + 1)}}; \quad (4)$$

the boiling crisis limit

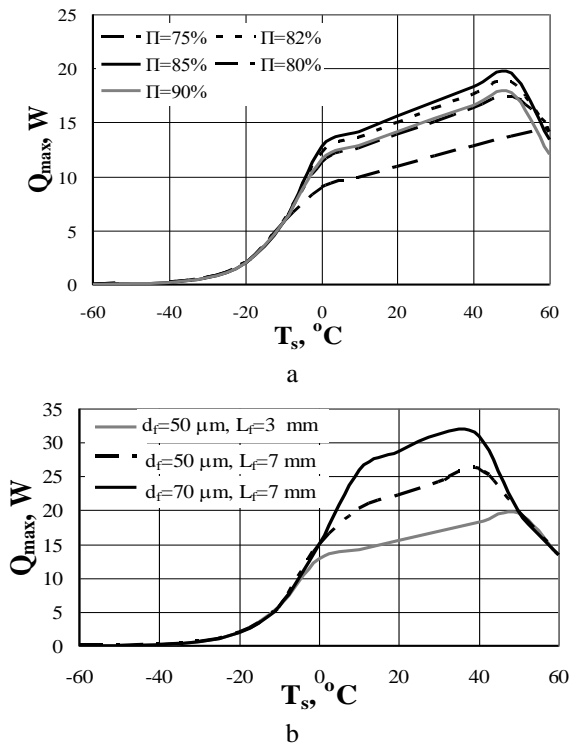
$$Q_{\max}^{\text{b}} = L_{\text{ev}} \frac{2\pi\lambda_{\text{eff}}^w T_s}{r\rho_v \ln\left(\frac{d_i^{\text{sh}}}{d_{\text{vc}}}\right)} \left( \frac{2\beta}{r_{\text{cr}}^{\text{b}}} - P_c \right), \quad (5)$$

where

$$\lambda_{\text{eff}}^w = \Pi\lambda_1 + (1 - \Pi)\lambda_m^w; \quad (6)$$

$r_{\text{cr}}^b$  - the critical radius of the vapor bubble at the nucleate boiling, m.

Results of maximum heat transfer ability calculation for the VCHP type A in the horizontal operational mode are presented on fig. 4.



a -  $d_f = 50 \mu\text{m}$ ,  $L_f = 3 \text{ mm}$ ; b -  $\Pi = 85\%$   
 Fig. 4. Choosing of the optimal wick parameters.

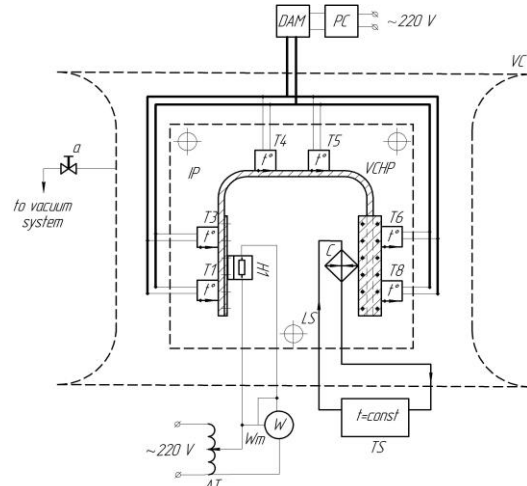
As it shown on fig. 4a for fiber diameter  $50 \cdot 10^{-6}$  m and fiber length  $3 \cdot 10^{-3}$  m maximum heat transfer ability at saturation temperatures above  $0^\circ\text{C}$  is provided by the wick with porosity 82...85%. For other values of  $d_f$  and  $L_f$  results were similar. That's why as final value was chosen porosity of 82...85%.

Fig. 4b depicts the choosing of optimal  $d_f$  and  $L_f$  for the wick with porosity 85%. The heat transfer ability at saturation temperatures below  $-20^\circ\text{C}$  is extremely low and in the temperature range  $-60^\circ\text{C} \dots 0^\circ\text{C}$  is specified by the sonic limit, at  $0^\circ\text{C} \dots +40^\circ\text{C}$  - the hydrodynamic limit, at  $+40^\circ\text{C} \dots +60^\circ\text{C}$  - the boiling crisis limit. Maximum heat transfer ability at saturation temperature above  $0^\circ\text{C}$  was provided by  $d_f = 70 \cdot 10^{-6}$  m and  $L_f = 7 \cdot 10^{-3}$  m and these values were chosen as final.

Calculation results for the VCHP type B were similar.

#### 4. EXPERIMENTAL SETUP

The HPL KPI experimental setup for investigation of the operational characteristics of both types VCHPs and for the start-up tests is shown on fig. 5.



VCHP - variable conductance heat pipe; H1 - heater; AT - autotransformer; Wm - wattmeter; T1-T8 - thermocouples; C - condenser; TS - thermostat; VC - vacuum chamber; DAM - data acquisition module; PC - personal computer; IP - installation platform; LS - leveling screws

Fig. 5. Experimental setup for VCHP testing.

The experimental setup (fig. 5) consisted of the heating and cooling systems, the temperature control and the vacuum system.

The heating system included the ohmic heater H1, the wattmeter Wm for the input power controlling and the autotransformer AT for the input power regulation. The heater H1 was screwed to the VCHP heat input zone flange through a graphite foil to reduce the contact heat resistance. Foils were used also to attach the condenser C to the heat output zone.

Cooling of the VCHP heat output zone was provided by means of the thermostat TS in testing at the positive operating temperature and by means of liquid nitrogen - at negative temperatures and in the start-up tests.

To reduce the heat losses into the environment all zones of the VCHP were covered by the multilayer insulation (MLI).

The VCHP temperature distribution was controlled by the T-type thermocouples T1-T8, which were mounted on the HP outer surface: three

in the heat input zone, two in the adiabatic zone and three in the heat output zone. Thermocouples signal through a data acquisition module DAM was transferred to the personal computer PC. Special software was used for the temperature measurements and recording in real time.

## 5. RESULTS OF HPL KPI VCHPs TESTING

### 5.1 Operational characteristics

Results of the thermal conductance testing are presented on fig. 6.

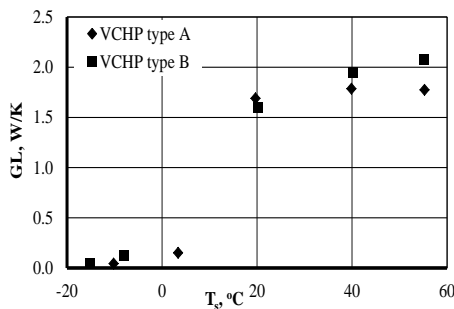


Fig. 6. Thermal conductance of the VCHPs.

The thermal conductance of both types VCHP is extremely low at temperatures below 0°C (0.04...0.15 W/K) and rises to the maximal values (1.8...2.1 W/K) with the temperature rising from 0 to 55°C (fig. 6). I.e. both types of VCHP have low heat transfer characteristics at negative temperatures and high – at the positive as it was predicted by the calculations. Thus variable conductance effect was reached by optimizing of the wick characteristics for the chosen heat carrier.

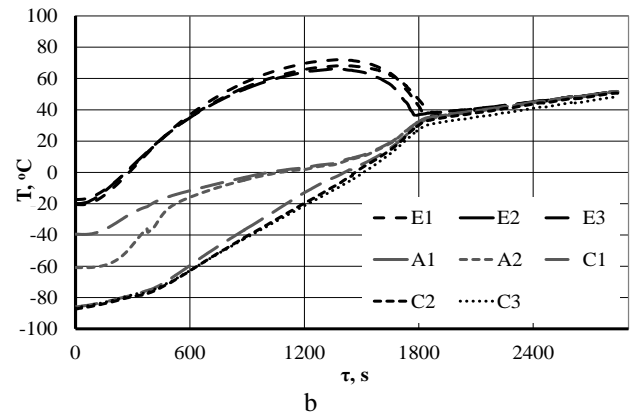
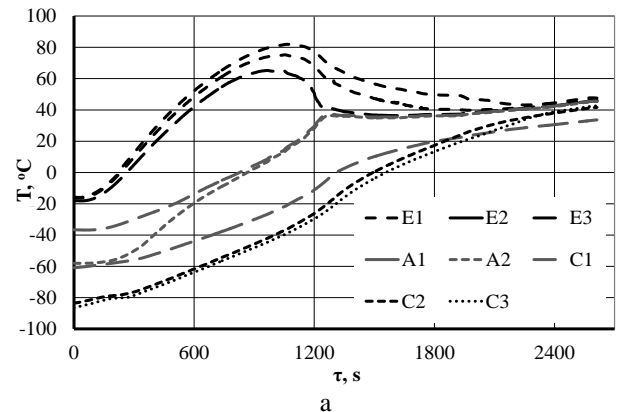
Both VCHPs transferred the heat power 10 W predicted by the MASCOT project conditions at the temperature range from +20°C to +55°C.

### 5.2 Start-up time

Results of start-up testing are presented on fig. 7.

The start-up tests were provided at the heat input 10 W and starting temperature of the condenser zone -85°C, which was maintained by means of liquid nitrogen. At the same time with the beginning of heat input the supply of liquid nitrogen was stopped. Start-up moment was indicated by decreasing of evaporator zone temperature, which was the evidence of heat transfer beginning between the evaporator and the condenser zones. The VCHP type A started after about 1100 s from the beginning of the heat input (fig. 7a) and the VCHP type B – about 1400 s (fig. 7b). Thereafter, the temperature difference between the evaporator and condenser

zones set at the level not exceeded 1.8 °C for the VCHP type A and 2.5°C for the VCHP type B, which was indicated the effective work of the HPs.



a – VCHP type A; b – VCHP type B;  
E1-E3 – temperatures in heat input zone; A1-A2 – temperatures in adiabatic zone; C1-C3 – temperatures in heat output zone

Fig. 7 Start-up time of VCHPs.

## 6. RESULTS AND DISCUSSION OF THE DLR TESTS IN THE WIDE TEMPERATURE RANGE

The Engineering, Qualification, Flight and Spare Flight Models were examined on the test bed of the Institute of Space Systems/DLR in order to obtain the latest information about the VCHPs characteristics before their integration into the TCS at adequate test conditions. The VCHPs performances were investigated inside the wide range of the heat fluxes (0.4...20 W) and condenser temperatures (-70°C...+60°C) with the detailed steps of their changing in order to collect sufficient information for their analytical re-presentation.

The test plan includes different geometries: 1D (the straight-line), 2D (bending in one plane in similar manner as the Flight HP) and the 3D Flight and Qualification configuration. 1D geometry test confirmed the principle of the temperature

regulation; the 2D test has demonstrated their transport ability in the condition of the minimal effect of Earth gravity; the 3D test showed the HP performance under the gravity condition in the reflux mode, in the orientation, similar to the thermal vacuum test with the whole TCS (gravity assisted).

All tests were conducted in vacuum, the VCHPs were mounted on the mounting plate (fig. 8) with regulated temperature and enclosed by the thermal shield which temperature equals to the mounting plate one. Special measures have been undertaken to layout HPs into horizontal plane (for 2D), to minimize the heat exchange between the HP and the thermal shield via the insulation, the heater and the sensors wires, the supports.

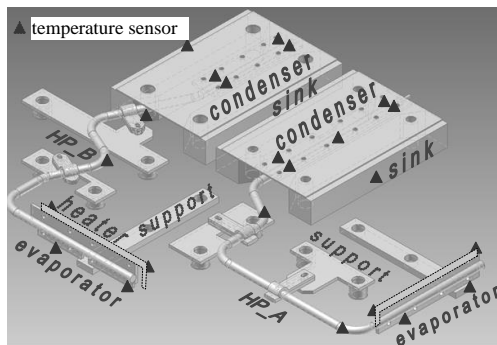


Fig. 8. 2D heat pipe arrangement on test bed. Thermal shields, single layer insulation, wires and mounting plate are not shown.

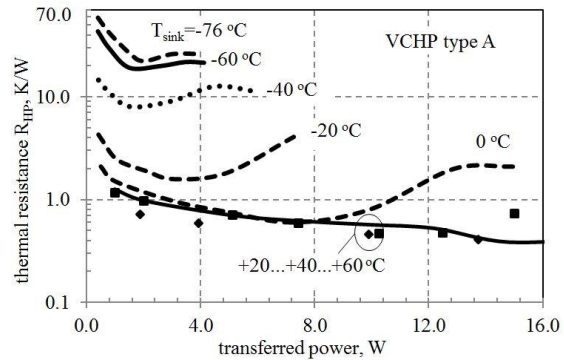
The typical HP performance characteristics are featured by the following dependence – at the lowest heat sink temperature and the lowest heat input power the thermal resistance reaches 40...70 K/W (similar as the resistance of the empty shell) and at the highest temperature and power shifts to values 0.3...0.5 K/W (similar to the conventional HP) (fig. 9a, b). The investigations of all geometries confirmed the variable properties which are the function of the transferred heat power and heat sink temperature.

The resistance uncertainty for the HPs mode at  $T_{\text{sink}} = -20...+60^{\circ}\text{C}$  is  $\pm 0.16$  (the minimal power) to  $\pm 0.11$  (the maximal power). For the switch off mode it is  $\pm 0.12$  to  $\pm 0.04$  ( $T_{\text{sink}} = -76...-40^{\circ}\text{C}$ ).

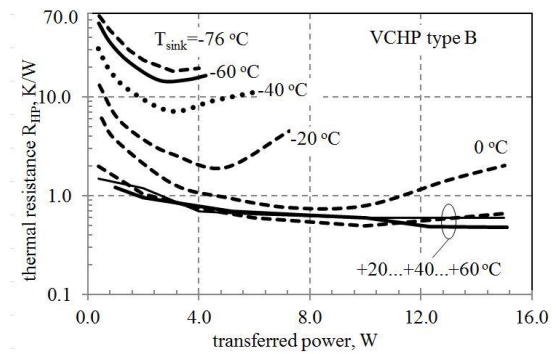
## 7. THE HEAT PIPE MODELLING AS THE PART OF THE TCS

Being the elements of the TCS the heat pipe should be correspondently presented in used TCS thermal model, to be solved by the thermal analysis software like ESATAN -TMS, Sinda, Thermica and other finite difference and finite elements software. The survey of the methods of the HP re-representation

and the tasks to be solved for this are collected in [8-10] and the individual software user manuals.



a



b

Fig. 9. Function of heat pipe thermal resistance (value is reverse to conductance) for 3D configuration from transferred power at different heat sink temperatures. Courtesy of DLR.

Issues related to introducing the HP into the elaborated TCS thermal mathematic model are: individuality of the HP thermal characteristics, manufacturing variations, strong impact of the wick and liquid, very diverse impact of the thermal boundary conditions and the HP design parameters combination (lengths, diameters, limitations). For most HPs, the inner heat transfer coefficients are not evident functions of the temperature difference “wall - vapor” and the heat flux density. They could be obtained mainly on the base of experimental data processing. In fact the user should include into the analyzer the representative and verified HP physical model. In most cases this is impossible as the manufacturer has no such one.

One of the time-effective and reliable way to fulfill the thermal modeling on the system level is to include the heat pipe(s) as element with known thermal conductance, parametrically dependable on the most essential boundary conditions. These functions are evaluated experimentally or analytically for the already defined HP design in whole range of the varying parameters. This

method was used for the MASCOT TCS mathematic model creation on the stage of finalization of the TCS design.

The model of the MASCOT TCS was developed in ESATAN-TMS. The heat transfer was considered adiabatic (no radiative exchange, as the external parts of the heat pipes are nickel coated with low solar absorptance and emissivity) between the evaporator and condenser, though only a geometrical model for the condenser and evaporator was implemented (based on their geometrical size). The performances measured via the thermal vacuum testing by DLR and interpretation of the results, for the multiple temperature values and the heat input (simulated by the heaters) were then used to model the variability effect. These results were collected in the tables based on the the HPs model (1D, 2D, 3D) as a calculated GL value between the temperature sensors positioned on the endings of the evaporator and condenser flanges during the tests. The values were then summarized as a function of the condenser temperature and heat power as input (Table 2).

Table 2. GL matrix for the heat pipes tested (for HP A).

P_HPA [w]	0.0	0.5	1.0	2.0	4.0	7.0	10.0	15.0	20.0
TCHPA [C]	GLHPA [w/K]								
-100	0.017								
-70	0.017								
-65	0.024	0.024	0.045	0.038					
-58	0.023	0.023	0.052	0.047					
-38	0.069	0.091	0.125	0.079					
-17	0.233	0.405	0.526	0.633	0.245				
0	0.478	0.663	1.039	1.324	1.670	1.244	0.478		
10	0.478	0.663	1.039	1.324	1.670	1.244	0.478		
25			1.036	1.426	1.692	2.162	1.364		
45			1.021	1.430	1.624	1.757	2.600	2.345	
100			1.385	1.708	2.178	2.178	2.454	2.454	

The values previously summarized were then introduced in the MASCOT lander thermal model via a specifically developed sub-routine based on a two-dimensional interpolation with the heat load on the evaporator and the condenser temperature as the inputs, GL as the output.

The performances can then be summarized in a graphical way for the two HPs as in fig. 10.

Only some small changes to the previously presented values had to be implemented in the ESATAN-TMS model in order to avoid instability issues during the simulations (in general curve derivatives and spikes to be smoothed).

In the previous graphs, “low” and “high” limits refer to the minimum and maximum heat transfer level at which the HPs were tested (function also of the temperature level on the heat sink).

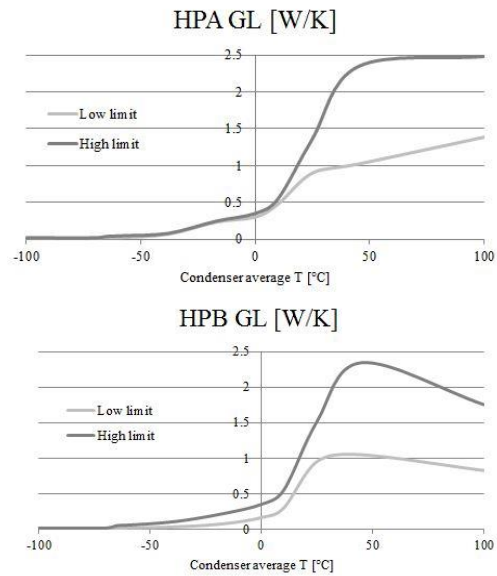


Fig. 10. GL calculated value for both heat pipes in MASCOT.

## 8. CONCLUSIONS

The decision to adopt the VCHP technology (selected as a trade-off of the possible variable heat transfer technologies) for the MASCOT lander TCS solved some issues related to the competitive technologies, such as reduction of the TCS mass and volume, absence of the active control. The heat exchange limitations with the space craft, the direct exposure to the external environmental conditions during the cruise phase (condition completely different from the one close to the asteroid surface and on it) and the limited heating power were the main issues in the design phase. The core of the thermal control system was represented by the developed variable conductive heat pipe system which is able to minimize the heat exchange with the exterior during cruise phase and maximize it on the asteroid surface.

The VCHP ON/OFF switchable operation mode was reached by choosing methanol as heat carrier and the structural parameters of the wick: fiber length and diameter, pore diameter, porosity, permeability.

The experimental investigations and tests of the Engineering, Qualification, Flight and Spare Flight Models showed that the VCHP performance characteristics were featured by the following dependence – at the lowest heat sink temperature and the lowest heat input power the thermal resistance reached 40...70 K/W (similar as the resistance of the empty shell) and at the highest temperature and power it shifted to values between 0.3...0.5 K/W (similar to the conventional VCHP).

Such flexibility of the VCHP system resulted also in a very good adaptation of the performances not only for the extreme conditions, but also for the temporary switch ON for health checks during cruise.

Both VCHPs of the system transferred the heat power of 10 W predicted for the MASCOT conditions at the temperature range from +20°C to +55°C.

The thermal modelling approach adopted for the VCHPs characteristics, based on the results of the test campaigns performed, is on purpose simplified. Modelling the physical phenomena within the HPs, as the heat career behavior and its interaction with the metal shell and wick, were considered an overkill for the project objectives and though discarded as approach. The wide thermal tests conducted allowed to cover all the possible performance cases, leading to the possibility to implement a sub-routine based on a simple variable GL between the condenser and the evaporator covering all the modelling cases of the lander TCS.

The VCHPs are the part of the thermal control systems of the MASCOT in flight since December 2014. The telemetric data obtained in September 2015 showed that all temperatures satisfied the requirements and expectations.

## NOMENCLATURE

$d$	: Diameter (m)
$F$	: Cross section area (m <sup>2</sup> )
$GL$	: Thermal conductance (W/K)
$L$	: Length (m)
$N$	: Merit number (W/m <sup>2</sup> )
$P$	: Pressure (Pa)
$R$	: Thermal resistance (K/W)
$R_{\mu}$	: Universal gas constant, 8314 (J/(kmolK))
$r$	: Heat of vaporization (J/kg)
$T$	: Temperature (K, °C)
$Q$	: Heat power (W)

### Greek Letters

$\beta$	: Surface tension (N/m)
$\gamma$	: Adiabatic index
$\mu$	: Molar weight (kg/kmol)
$\lambda$	: Thermal conductivity (W/(m K))
$\Pi$	: Porosity (%)
$\rho$	: Density (kg/m <sup>3</sup> )
$\tau$	: Time (s, min, hour)

### Subscripts and Abbreviations

$ad$	: Adiabatic zone
$b$	: Boiling
$c$	: Capillary

$con$	: Condenser, heat output zone
$eff$	: Effective
$ev$	: Heat input zone, evaporator
$f$	: Fiber
$GLHP$	: Gas loaded heat pipe
$HP$	: Heat pipe
$hyd$	: Hydrodynamic
$i$	: Inner
$LHP$	: Loop heat pipe
$l$	: Liquid
$m$	: Material
$max$	: Maximal
$MLI$	: Multilayer insulation
$s$	: Saturation
$sink$	: Sink
$sh$	: Shell
$sn$	: Sonic
$TCS$	: Thermal control system
$TDHP$	: Thermal diode heat pipe
$VCHP$	: Variable conductance heat pipe
$v$	: Vapor
$vc$	: Vapor channel
$w$	: Wick

## REFERENCES

- [1] Reay D.A., Kew D.A., *Heat Pipes*. Fifth edition, Butterworth-Heinemann is an imprint of Elsevier, (2006).
- [2] Thienel L., Lewis M.R., Brennan P.J., et. al., *Design and performance of the cryogenic flexible diode heat pipe (CRYOFD) Flight experiments. Final report*, Jackson and Tull Space&Aeronautics Technology Division, (1998).
- [3] Kayaa T., Goncharov K., Investigation of the thermal performance characteristics of a variable conductance arterial heat pipe, *Frontiers in Heat Pipes (FHP)*, 013004 (2011).
- [4] Maydanik Y.F., Loop heat pipes, *Applied Thermal Engineering*, Vol. 25 (2005), 635–657.
- [5] Baturkin V., Zhuik S., Savina V. Development and research of heat pipes for thermal control system of scientific apparatus, *IV international seminar t. Frunze*, Moscow, USSR (1989) 201–208.
- [6] Semena, M.H. Gershuni, A.N., Zaripov, V.K., *Heat pipes with metal-fibrous capillary-porous structures*, High school. (1984) 215 p.
- [7] Chi, S.. *Heat Pipe Theory and Practice: A Sourcebook*, McGraw-Hill, (1976) 242 p.
- [8] Baturkin V. Simulation of temperature regimes of heat pipes in thermal control systems of space instrumentation by finite element method, *Proc. of 11-th Int. Heat Pipe Conf. Preprint Vol. 2*, Musashinoshi, Tokyo, Japan (1999) 210–215.
- [9] Cullimore B, Baumann J., FDM/FEM System-level Analysis of Heat Pipes and LHPs in Modern CAD Environments, *16 Aerospace Thermal Control Workshop*, El Segundo, California (2005).
- [10] Baturkin V., Thermal control systems with variable conductance heat pipes for space application: theory and practice, *Heat pipes and solid sorption transformations: fundamentals and practical applications*, CRC Press Taylor&Francis Group (2013).